Received: 10 March 2019 | Revised: 16 May 2019 | Accepted: 6 June 2019

DOI: 10.1002/ese3.395

RESEARCH ARTICLE

Energy Science & Engineering Open Access

Numerical analysis of particle erosion in the rectifying plate system during shale gas extraction

Shanbi Peng[1] | **Qikun Chen**[1] | **Congxin Shan**[2] | **Di Wang**[3]

[1]School of Civil Engineering and Architecture, Southwest Petroleum University, Chengdu, China

[2]Natural Gas Research Institute, Southwest Oil and Gas Field Branch, Chengdu, China

[3]Beijing Oil and Gas Pipeline Control Center, CNPC, Beijing, China

Correspondence
Shanbi Peng, School of Civil Engineering and Architecture, Southwest Petroleum University, Chengdu 610500, China.
Email: shanbipeng@swpu.edu.cn

Funding information
Applied Basic Research Program of Sichuan Province, Grant/Award Number: 2019YJ0352; Sichuan Provincial Natural Resources Research, Grant/Award Number: KJ-2019-11

Abstract

Erosion caused by sand particles in the pipe system is a major concern in the shale gas industry. In the rectifying plate system, the fluid with high Reynolds number is assumed to be the fully turbulent flow. To investigate particle erosion under the complex flow in the rectifying plate system, various erosion simulations are conducted in this study. Because the gas velocity, sand input, particles size, and particles shape can affect the erosion in rectifying system, the effect of gas velocities (5-30 m/s), sand inputs (50-400 kg/d), and particle parameters (various particle sizes and various particle shapes) on erosion is simulated. Moreover, the erosion experiment conducted in Tulsa University is used to verify the accuracy of simulation model. Through the calculation and analysis, it is obtained that different gas velocities will change the position where the max erosion rate appears. Various sand inputs lead to different max erosion rates. In addition, the effect of sand input on the distribution of erosion scars on rectifying plate is more obvious than that of on elbows. Finally, the effect of size and shape of particles on erosion is investigated. It is found that with the increase in particle diameter, the shape of erosion scar on elbow 1 changes gradually from an ellipse to the V-shape.

KEYWORDS

computational fluid dynamics (CFD), particle erosion, rectifying plate system, shale gas extraction

1 | INTRODUCTION

Sand particles are the primary cause leading to pipe erosion in the shale gas industry. In the early stage of shale gas extraction, the max sand rate in the gas pipe is high to 10 tons/d. The sand separator is generally used to remove the sand particles in order to guarantee the purification of shale gas. Then, the purified shale gas comes into the rectifying and measuring devise before exporting of shale gas. However, sand particles will enter gas pipes when the separator breaks down. High gas velocity leads to high velocity of sand particles which may cause erosion or deformation in pipes. The rectifying plate at the front of the flowmeter is always installed to stabilize the fluid.[1] Peng et al[2] studied the function of the rectifying plate numerically and indicated that it can stabilize the fluid in the gas pipe. There are many researchers studied the erosion in the elbow of pipes but only a few have studied the erosion in different valves. Though the erosion in rectifying plates cannot be ignored, it is still not drawn much attention.

The computational fluid dynamics (CFD) method is widely used to analyze the erosion causes in recent years. In studies of erosion, the CFD method helps capture

particle trajectories and can calculate the erosion rate. Duarte et al[3] used the CFD method to study the erosion and found an optimum method that using spiral internal structure can effectively reduce the erosion degree. Pei et al[4] simulated the erosion in pipe elbows and have given the position of maximum erosion; the abrasive terms in erosion simulation are proved necessary, and the particle impact angles are generally low in transportation of dense gas.[5] Peng et al[6] studied the particle trajectories in erosion simulation by combining eight erosion models and two rebound models, and have found the prediction of the maximum erosion zone in this paper; Laín et al[7] studied the bend erosion with the approach of Euler/Lagrange and found that the roughness of wall can reduce the penetration ratio; Zeng et al[8] used the CFD-DEM coupling way to study the motion of sulfur particles in the gas flow; Liu et al[9] used CFD to study the diffusion rule of two different oils in tee pipe; Duarte et al[10] studied the relationship between collision of interparticles and the elbow erosion with the numerical simulation; Vieira et al[11] combined the PIV technique and the sand erosion experiment, then simulated the erosion and gave the prediction of erosion; in the study of Duarte et al[12] the particle erosion in the pipe elbow was investigated, and the conclusion indicated that the collision of inner particles can effectively reduce the erosion in the elbow.

Experiments have been always an effective method to study the particle erosion; Wong et al[13] used the experiment method to study the process of erosion in cavity of a pipe. The experiment which was conducted in Tulsa University[11] was quoted in some researches for great credibility, and authors indicated that "V-shape" erosion occurred in the pipe elbow through the CFD simulation.

Comparing with the study of the pipe erosion, the study of erosion in equipment in the pipe system is much less. Liu et al[14] studied the erosion in the butterfly valve in a pipe and validated it with the experiment; Yin et al[15] simulated the erosion in hydraulic spool valves and evaluated the life of the equipment; Zhu et al[16] simulated the flow erosion of the needle valve and investigated the effect of valve sizes, particle concentration, and fluid parameter on the erosion rate; Messa et al[17] used the CFD method which contains the Euler-Euler approach and Euler-Lagrange approach to evaluate the erosion in the needle valve and indicated that this new method can reduce the burden of the computational calculation for the particle tracking and the erosion estimation.

There are various erosion cases among those studies while only a few studies about the erosion in the rectifying plate can be found. However, all these erosion cases which contain data of experiments and simulation models are useful in describing erosion characteristics.

2 | MATHEMATICAL MODEL

2.1 | Model of fluid phase

In the simulation, kinetic energy of turbulence (k) and turbulent dissipation energy (ε) is used to restrict turbulent fluctuation.[18]

$$U_j\frac{\partial k}{\partial x_j}=\frac{\partial}{\partial x_j}\left(\frac{v_t}{\sigma_k}\frac{\partial k}{\partial x_j}\right)+v_t\left(\frac{\partial U_i}{\partial x_j}+\frac{\partial U_j}{\partial x_i}\right)\frac{\partial U_i}{\partial x_j}-\varepsilon \quad (1)$$

$$U_j\frac{\partial \varepsilon}{\partial x_j}=\frac{\partial}{\partial x_j}\left(\frac{v_t}{\sigma_k}\frac{\partial k}{\partial x_j}\right)+\frac{\varepsilon}{k}\left[C_{\varepsilon 1}v_t\left(\frac{\partial U_i}{\partial x_j}+\frac{\partial U_j}{\partial x_i}\right)\frac{\partial U_i}{\partial x_j}-C_{\varepsilon 2}\varepsilon\right] \quad (2)$$

2.2 | Model of erosion

Generally, the erosion rate is defined as the mass loss per unit area of wall material per unit time [kg/(m^2 s)] and the erosion can be calculated by analyzing the cumulative damage of each particle to the wall.

In the experiment of Tulsa University,[11] the erosion rate is defined as:

$$E_r=KF_sf(\alpha)\left(\frac{u_{rel}}{u_{ref}}\right)^n \quad (3)$$

where K is a constant about materials and the default value for steel is 2×10^{-9}; $f(\alpha)$ is the impact angle function of particle; u_{ref} is the constant of particle reference velocity;

Haugen et al[19] indicated that erosion rate can be described as:

$$E_r=Kf(\theta)\left(\frac{u_{rel}}{u_{ref}}\right)^n \quad (4)$$

where $f(\theta)$ is the impact angle function of particles, which is:

$$f(\theta)=A\theta+B\theta^2+C\theta^3+D\theta^4+E\theta^5+F\theta^6+G\theta^7+H\theta^8 \quad (5)$$

where A, B, C, D, E, F, G, and H are constant which obtained by calculation.

Value of θ is from 0 to $\frac{\pi}{2}$ rad.

Nelson and Gilchrist[20] conducted an experiment and obtained the erosion equation:

$$e_r=e_{rC}+e_{rD} \quad (6)$$

where e_{rC} is the cutting erosion; e_{rD} is the deforming erosion.

$$e_{rC}=\begin{cases}\dfrac{u_{rel}^2\cos^2\alpha\sin\frac{\pi\alpha}{2\alpha_0}}{2\varepsilon_C},\alpha<\alpha_0\\ \dfrac{u_{rel}^2\cos^2\alpha}{2\varepsilon_C},\alpha\geq\alpha_0\end{cases} \tag{7}$$

where α_0 is the user-defined conversion angle, and the ε_C is the user-defined shear coefficient.

$$e_{rC}=\frac{max\left(u_{rel}\sin\alpha\right)}{2\varepsilon_D} \tag{8}$$

where ε_D is coefficient of deformation, and K is a value of velocity of cutting.

Oka et al[21] described the erosion as:

$$e_r=e_{90}g\left(\alpha\right)\left(\frac{u_{rel}}{u_{ref}}\right)^{k_2}\left(\frac{D_p}{D_{ref}}\right)^{k_3} \tag{9}$$

The function of angle is defined as:

$$g\left(\alpha\right)=\left(\sin\alpha\right)^{n_1}\left(1+H_v\left(1-\sin\alpha\right)\right)^{n_2} \tag{10}$$

where n_1, n_2, and H_v are user-defined constants. H_v is the Vickers hardness.

D_{ref} is the diameter of particle which can be defined by users.

In the literature of Jeremy et al[22] the erosion rate is defined as:

$$ER=1.559e^{-6}B^{-0.59}F_s v f\left(\alpha\right) \tag{11}$$

where ER is the erosion rate, B is the Brinell hardness. F_s is the factor of shape. The complete spherical particle is 0.2, the hemispherical particle is 0.5, and the irregular particle is 1.

The impact angle function can be fitted by piecewise linear function. The following is an impact angle function of sand particle erosion in steel:

$$f\left(\alpha\right)=\begin{cases}0+22.7\alpha-38.4\alpha^2,\alpha<0.267rad\\ 2.00+6.80\alpha-7.50\alpha^2+2.25\alpha^3,\alpha\geq0.267rad\end{cases} \tag{12}$$

In ANSYS software, DPM model of Fluent can be chosen to solve the erosion problem. Moreover, the simulation for particle erosion is relatively simple and defined as:

$$E_{erosion}=\sum_{p=1}^{N_{particle}}\frac{\dot{m}_p C\left(d_p\right)f\left(\alpha\right)v^{b(v)}}{A_{face}} \tag{13}$$

where:

$C\left(d_p\right)$ is the diameter function of particle;
α is the impact angle;
$f\left(\alpha\right)$ is the function of impact angle;
V is the relative velocity of particle;
$b\left(v\right)$ is the function of particle relative velocity;
A_{face} is the area of wall surface.

And, it is essential to define the rebound coefficients in FLUENT software; Grant and Tabakoff et al[23] proposed the equations by experiment and calculation which are used in this study and can be written as:

$$e_n=0.993-1.76\alpha+1.56\alpha^2-0.48\alpha^3 \tag{14}$$

$$e_n=0.998-1.66\alpha+2.11\alpha^2-0.67\alpha^3 \tag{15}$$

However, different erosion models need different parameters, for the boundary condition will vary from cases to cases, so the default parameters cannot suit for each erosion model. Therefore, the real value of these parameters should be given in practical applications.

3 | METHODOLOGY AND VALIDATION

3.1 | Models of pipe and rectifying

The structure of the rectifying plate system is shown in Figure 1. It consists of 19 holes that allow gas fluid to flow through and help stabilize the fluid. Sizes of each component and radius of curvature are given after field measurement in Changning shale gas station (Sichuan Province, China).

As shown in Figure 1, the case that sand particles escape from the separator and enter into the pipe system (from A to B) is studied. With the gas flowing, the sand particles will get into the rectifying plate. In order to investigate the erosion, CFD method is used. Because the fluid inside the pipe is the calculation zone, the Boolean operation is used for removing the extra parts.

The model and mesh are generated by ANSYS Workbench, as shown in Figure 2, 579200 grids are generated, and the inflation method is used to make simulation of flowing closer to practical.

3.2 | Validation and analysis

The results of numerical simulation may be different due to the fineness of the mesh and the choice of the algorithm. In this study, the experiment and simulation conducted by Vieira et al[11] in Tulsa University are referred to validate the simulation result.

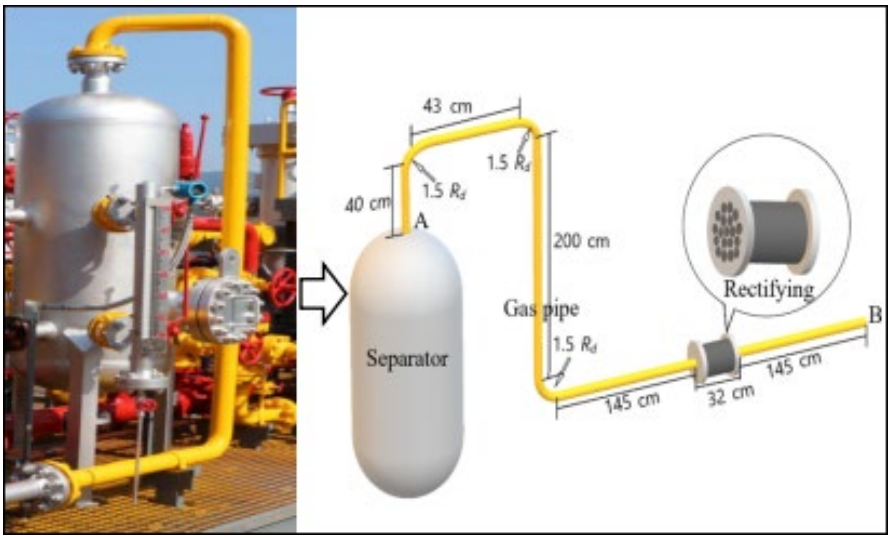

FIGURE 1 Instruction of the rectifying plate system

First, the verification of the grid independence is conducted, the grid numbers of 579200, 836502, 1104017, 1773785, and 4095597 are conducted, and the corresponding results are shown in Table 1 and Figure 3.

It can be thought that the model with the grid number of 579200 can meet the requirement. Moreover, the residual exponents of each term are under 10^{-4} and the mass conservation is satisfied. Then, the simulation is validated with the erosion experiment of Tulsa University. In this experiment, sand particles are set as the injection with the flow rate of 227 kg/d, all particle diameters are uniformly defined as 300 μm, and the velocity of gas and particles are set as 23 m/s. The Standard k-ε model is applied as the turbulence model for simulation and the DPM model is used for solving the erosion rate. Turbulence intensity is set to 5%, and hydraulic diameter is set to 150 mm. Inlet is set to velocity boundary while outlet is set to pressure boundary. The enhanced wall treatment is used for better accuracy. In consideration of interaction between particles and eddies in fluid flow, the discrete random walk (DRW) model is applied in simulation. The result of erosion in the elbow is shown in Figure 4.

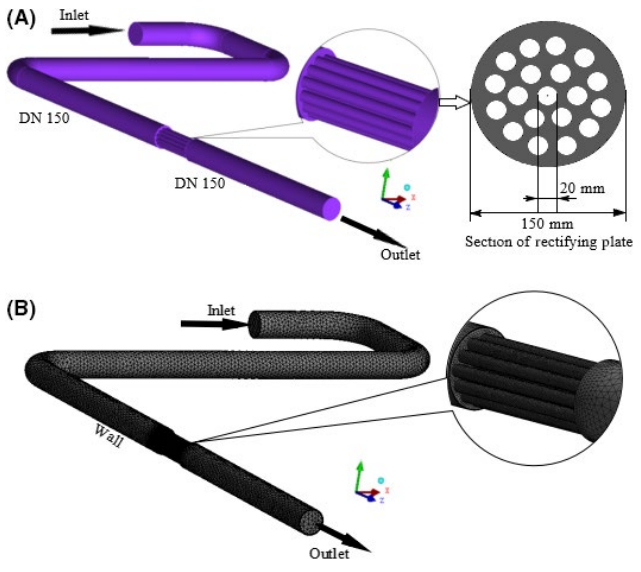

FIGURE 2 Generation geometry (A) of and mesh (B)

It can be seen from the simulation result that the "V-shape" of erosion is generated on the pipe elbow. The "V-shape" erosion scar is slightly different from that of the study.[10] It may be different according to the study of Solnordal et al.[22] In their research, the erosion shape is more like an ellipse because of different pipe structures.

On the other hand, in experiment of Tulsa University, the value of the erosion rate measured is 80.3 mm/y, and the maximum value of the prediction conducted by the CFD is 8×10^{-5} kg/m^2 s. Jie et al[3] simulated the pipe erosion by using the same boundary condition, and the value of the maximum erosion rate is 7.92×10^{-5} kg/m^2 s. In this paper, the max value of erosion rate is 6.31×10^{-5} kg/m^2 s.

Moreover, the status of flow field in pipe systems is simulated. Because the max flow rate appears in the rectifying plate, and this zone is tiny which makes the change of whole flow field seems not obvious, the range of velocity in result is adjusted between 0 and 30 m/s expected in zone of rectifying. Ten cross sections numbered from 1 to 10 are generated inside the pipe, and the result is shown as below in Figure 5 (unit of velocity: m/s).

It can be seen from Figure 5 that fluid flowed into the inlet and pass through each cross section then flowed out from outlet. Because of height difference between cross section 1 and cross section 5, fluid was accelerated by gravity. The bend between cross section 4 and cross section 5 changed the direction of fluid flow which increased the instability of flow. However, after passing through the rectifying plate, the fluid is stabilized and the velocity distribution of cross section 9 and cross section 10 became uniform. To investigate whether the fluid is fully developed, the Reynolds number of pipe section (cross section 5 to cross section 7) is calculated

TABLE 1 Verification of grid independence

Grid number	Maximum gas velocity (m/s)	Relative error	Maximum erosion rate (kg/m^2 s)	Relative error
579200	59.3	–	6.31×10^{-5}	–
836502	59.8	0.8%	6.28×10^{-5}	0.5%
1104017	57.1	3.7%	6.33×10^{-5}	0.3%
1773785	61.2	3%	6.16×10^{-5}	2.3%
4095597	60.3	1.6%	6.37×10^{-5}	0.95%

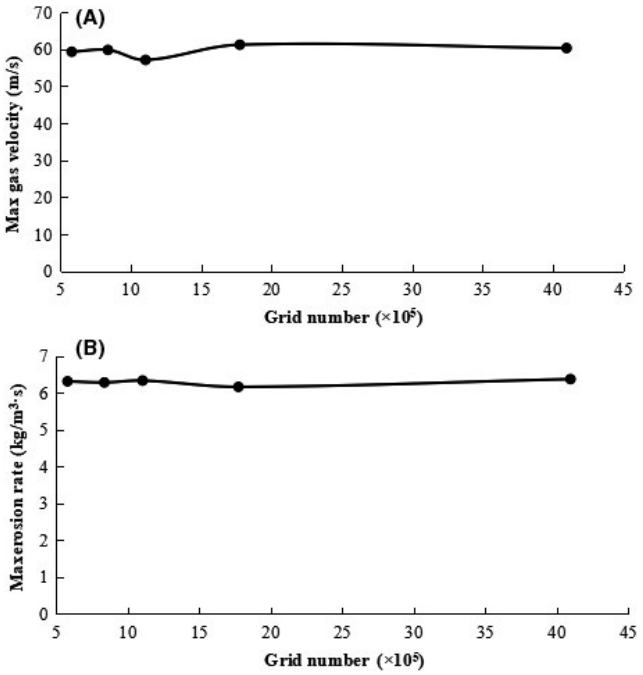

FIGURE 3 Verification of grid independence

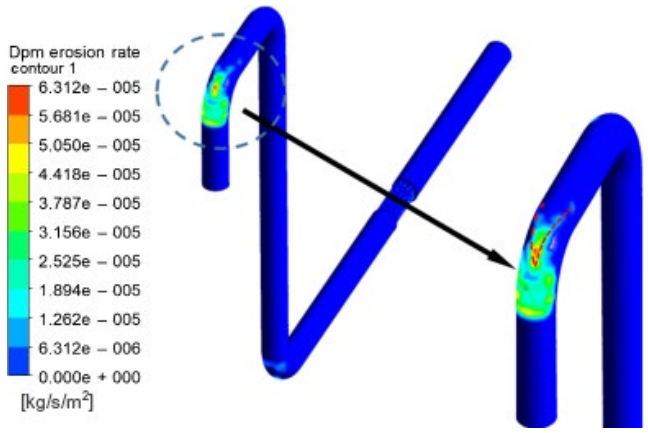

FIGURE 4 Erosion of simulation on pipe elbow

and the results are shown in Figure 6. Positive direction of transverse axis is the direction of fluid flow, and the "distance" is the horizontal distance from cross section 5. The density and viscosity of gas are 1.2 kg/m^3 and 1.8×10^{-5} kg/(m-s), respectively.

In Figure 6, the change of the Reynolds number can be observed clearly. With distance increasing from 0 mm to 40 mm, the Reynolds number has a slight increase. With distance increasing from 40 mm to 100 mm, the value of Reynolds number remains almost unchanged. However, when distance exceeds 100 mm, the Reynolds number increases rapidly. This is because this region is near the rectifying plate, and when fluid passes through this region, the flow flied will be affected. This result indicates that the fluid is fully developed before entering the rectifying plate. High Reynolds number of flow field illustrated that the fluid in rectifying system is fully turbulent which makes the particles motion more complex.

It can be obtained that the distribution of the fluid velocity becomes disordered when the fluid passes through the three elbows and becomes stable after passing through the rectifying plate. This result can describe the actual situation.

In conclusion, the model of the rectifying plate system can be assumed reliable.

4 | RESULTS AND DISCUSSION

The erosion in the rectifying plate system is a complex process. The impact angles of particles on the pipe elbow and the rectifying plate are different. The path line of particle motion in the pipe system and different position can be found in Figure 7.

Path lines of tracked particles can be directly observed in Figure 7. At position 1 and position 2, the particles rebound after hitting the elbow wall, and the particles trajectories are regular during the whole process. At position 3, due to the existence of the rectifying plate, some particles rebound when they hit the wall of the plate, and the other particles enter the bundles. Because of the small radius of the bundle, some particles with large incident angle occur multiple rebounds after entering the bundle of the rectifying plate. Hence, the erosion scar in the rectifying plate is different from that on elbows and the results of Figure 8 can prove it.

Particles hit elbow 1 first with large energy, hence the erosion strength is large in this position. Then the particles hit elbow 2. Because of energy loss, the erosion strength of elbow 2 is weaker than that of elbow 1. However, in elbow

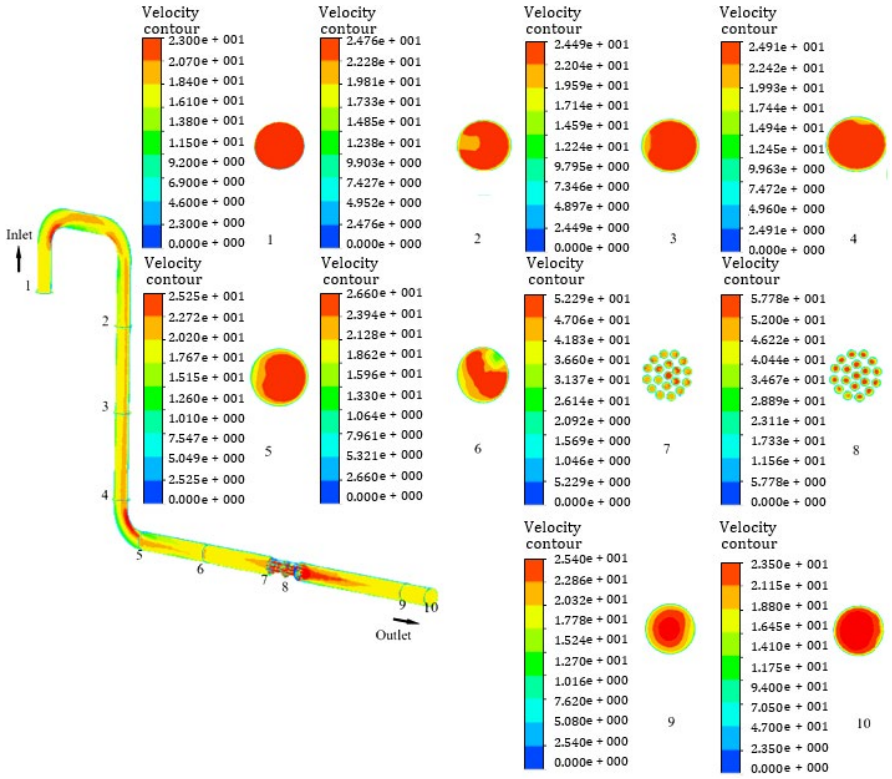

FIGURE 5 Flow field inside the rectifying plate system

3, the erosion degree is greater than that on elbow 2 because of gravity.

At position 3, the erosion scars are no longer a large area. Compared with erosion scars in position 1 and position 2, there are many erosion scars in position 3. Area of each erosion scar is small, but the erosion rate is high in this position. The flow path of the fluid changes near the entrance of the rectifying plate which leads to varying of the impact angle of particles.

4.1 | Erosion analysis at different gas velocities

In order to investigate the effect of the gas velocity on particles trajectories and erosion, different values of gas velocity are set in the simulation. As well, the flow rate of sand particles is set 227 kg/d which equals 0.0026 kg/s. Firstly, the erosion in rectifying plate system under low gas velocity (5-13 m/s) is simulated and the corresponding results are shown as below in Figure 9.

With gas velocity increasing from 5 m/s to 10.3 m/s, it can be obtained that the max erosion rate appears on the elbow 3 but not on elbow 1. Energy loss produced after particles pass through and hit the elbow 1 and elbow 2 though particles are accelerated by gravitational acceleration from position 2 to position 3. Because the initial velocity of particles is small, the influence of potential energy on particles erosion is more obvious than that of energy loss appears on position 1 and position 2. Hence, the max erosion rate appears on elbow 3. But when gas velocity exceeds

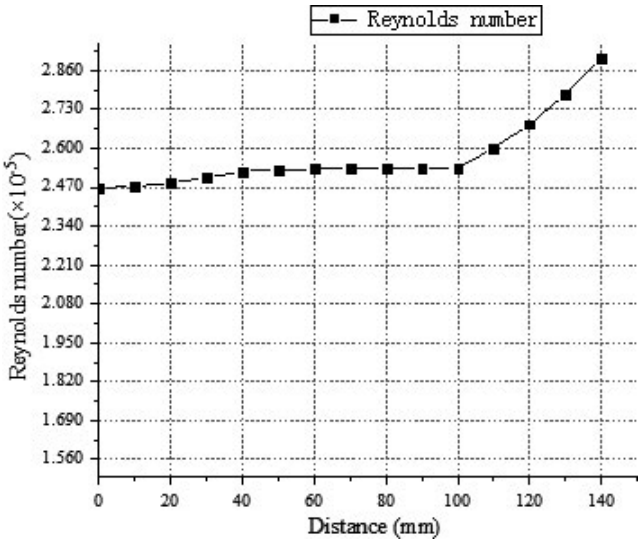

FIGURE 6 Reynolds number of fluid flow in pipe section

10.3 m/s, the influence of energy loss on particles erosion is more obvious and the Max erosion rate appears on elbow 1. However, as the gas velocity continues to increase, the law of erosion has changed. Erosion of rectifying plate with higher gas velocity (13-30 m/s) is simulated, and the results show as follow in Figure 10.

Figure 10 shows that when the velocity of gas increases from 13 m/s to 30 m/s, the distribution of erosion scars in elbows does not change very prominently, but the erosion rate increases. It is worth mentioning that when the velocity

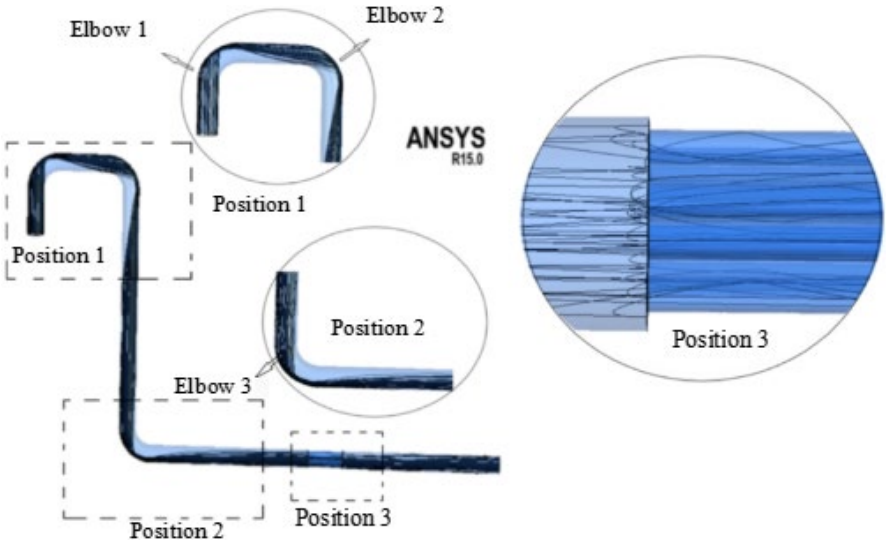

FIGURE 7 Particles trajectories in different positions

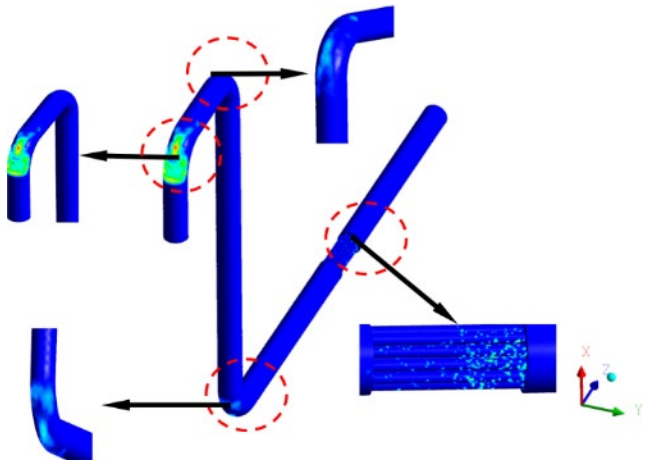

FIGURE 8 Erosion scars in different positions

is small, the maximum erosion zone appears at elbow 1 like (A) and (B), but when the velocity of gas is greater than 23 m/s, the maximum erosion zone appears on the wall of the rectifying plate. Though the area of the erosion scar is very small, it increases gradually with the increase in the gas velocity like (D) shows. This is because when gas flows into the rectifying plate with the high speed, the bundles with smaller diameter change the velocity vectors of fluid nearby, and the trajectories of particles will change as a consequence. Some particles hitting the wall of the rectifying plate with the large impact angle and high speed will increase the erosion rate. Moreover, the area of erosion scars in the rectifying plate is increasing with the increase in velocity.

The erosion rate of the gas velocity from 13 m/s to 30 m/s is simulated and analyzed. The results are shown as below in Figure 11.

Figure 11A shows the relationship between the gas velocity and the maximum erosion rate of whole system, and Figure 11B shows the maximum erosion rate on elbow and the rectifying plate, respectively. Three regions are divided and numbered with 1, 2, and 3 in the graph (A). In region 1, the maximum erosion rate increases slightly when the velocity increases from 13 m/s to 20 m/s. In region 2, the maximum erosion rate of whole system increases rapidly with the gas velocity increasing from 20 m/s to 23 m/s. And in region 3, the max erosion rate of whole system increases steadily. In the graph (B), two curves describe the maximum erosion rate on elbow 1 and the rectifying plate, respectively. There is an intersection P exists between two curves, and after calculation, the coordinates parameters of it is obtained as shown.

Hence, under the condition that the flow rate of sand particles is 0.0026 kg/s, when the velocity of gas increases from 13 m/s to 20.25 m/s, the maximum erosion zone appears on elbow 1, and when gas velocity exceeds 20.25 m/s, the maximum erosion zone should appear on the rectifying plate. In other words, the max erosion rate of elbow 1 and the rectifying plate can be used to predict the max erosion rate of whole system with different gas velocities, respectively.

4.2 | Erosion analysis at different sand inputs

In the process of the shale gas exploitation, the amount of sand carried by gas is not at constant flow rate which will lead to different erosion rates. In order to investigate the relationship between the sand input and the maximum erosion rate of system, the maximum erosion rate with various sand inputs is simulated. The gas velocity is set to 20.25 m/s in this section.

As shown in Figure 12, it can be observed that the maximum erosion rate of elbow 1 is increasing though the distribution of erosion zone does not obviously change. However, it is different on the rectifying plate. It can be observed from

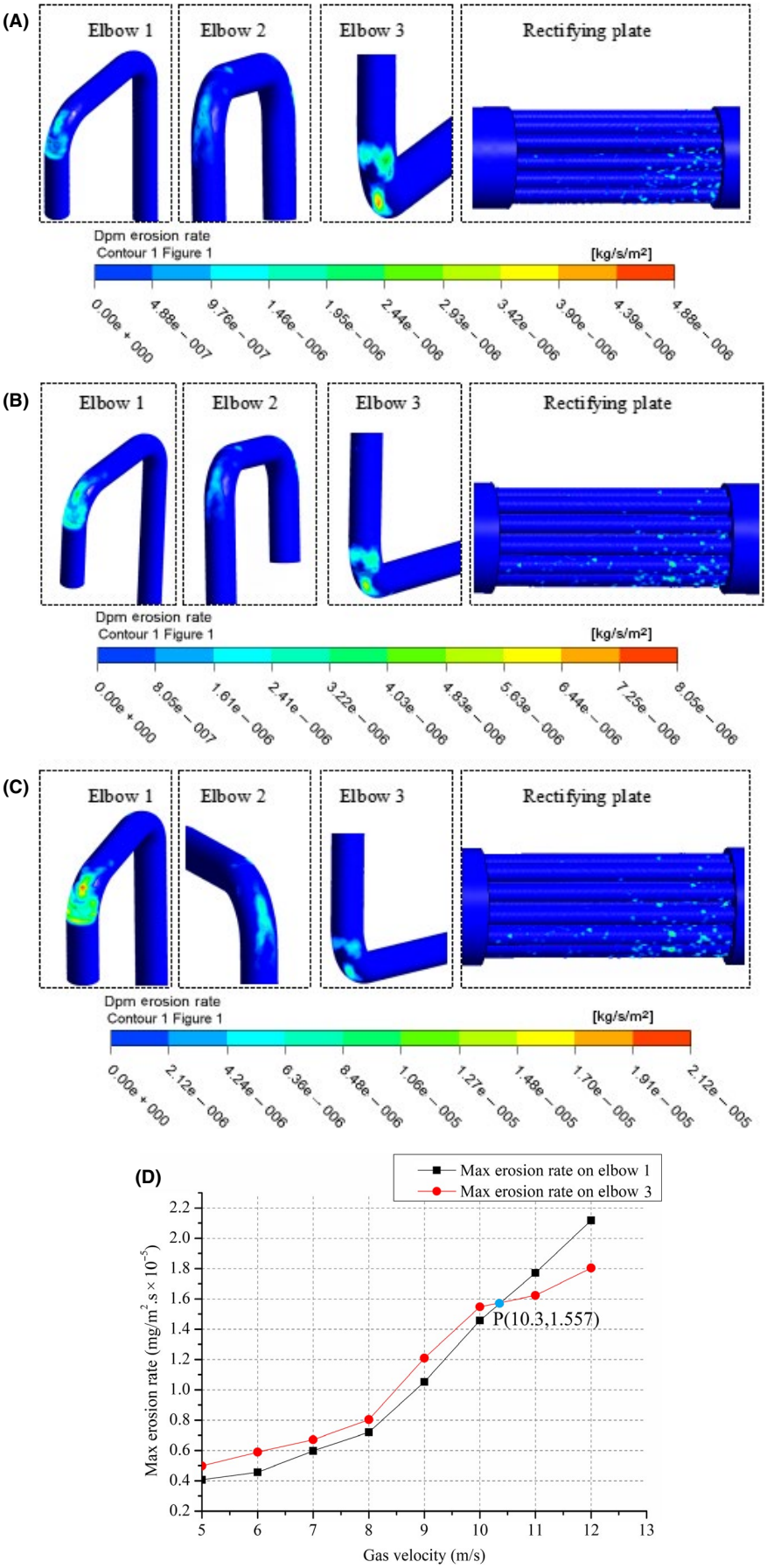

FIGURE 9 A, Erosion rate at gas velocity of 5 m/s. B, Erosion rate at gas velocity of 8 m/s. C, Erosion rate at gas velocity of 12 m/s. D, Maximum erosion rates of elbow 1 and the elbow 3

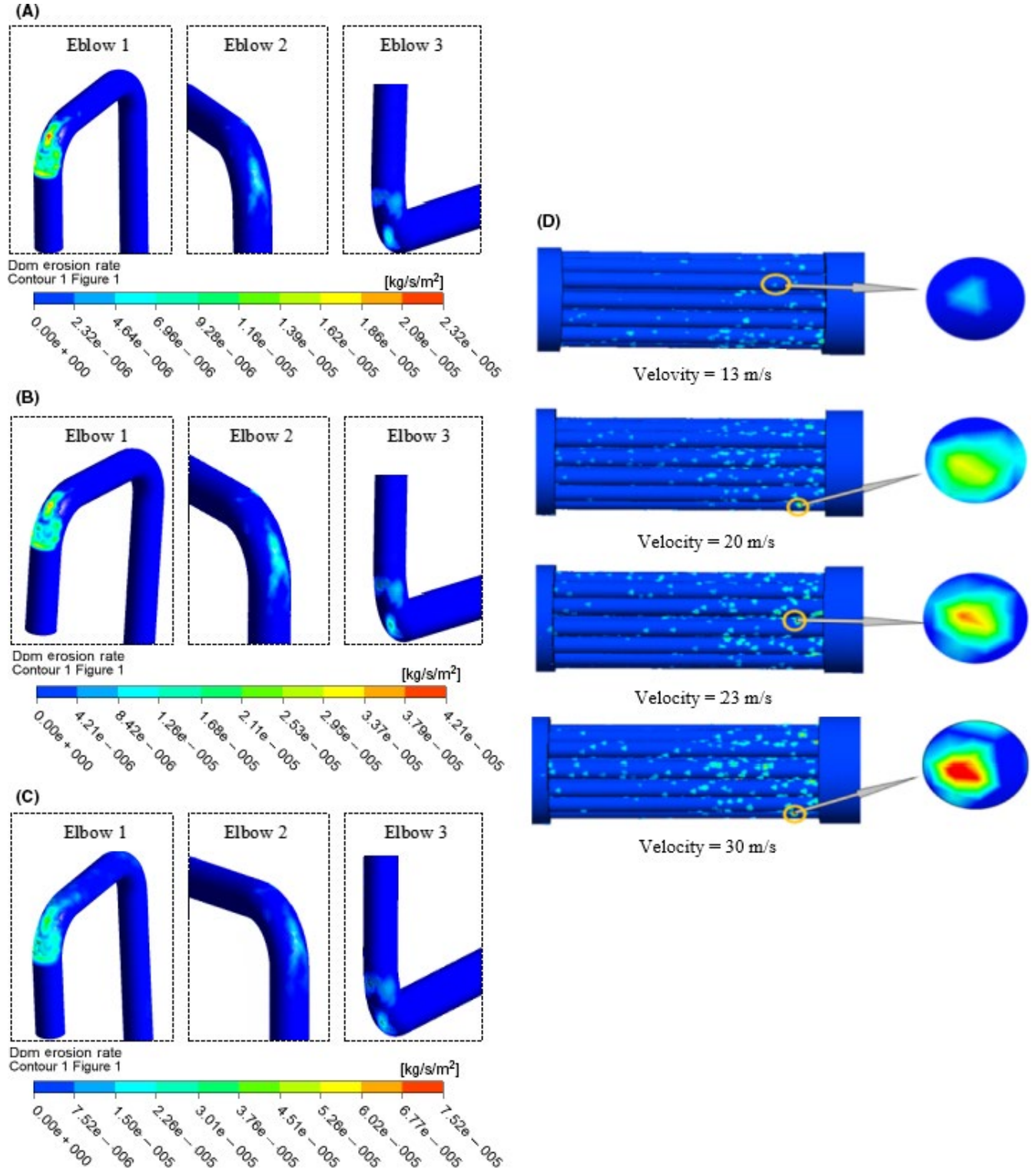

FIGURE 10 A, Erosion rate at gas velocity of 13 m/s. B, Erosion rate at gas velocity of 20 m/s. C, Erosion rate at gas velocity of 30 m/s. D, Erosion rate of rectifying at different velocities

(D) that with the change of the sand flow, both the distribution of erosion scars and max erosion rate changed. The reason for this phenomenon is that the trajectories of sand particles in the pipe are much more orderly than that in the bundles of the rectifying plate. With the increase in sand particles, more sand particles will enter and hit the rectifying plate at different incident angles.

In order investigate the influence of the sand input on pipeline erosion rate, various flows of sand particles set in the simulation, and the result is shown as below in Figure 13.

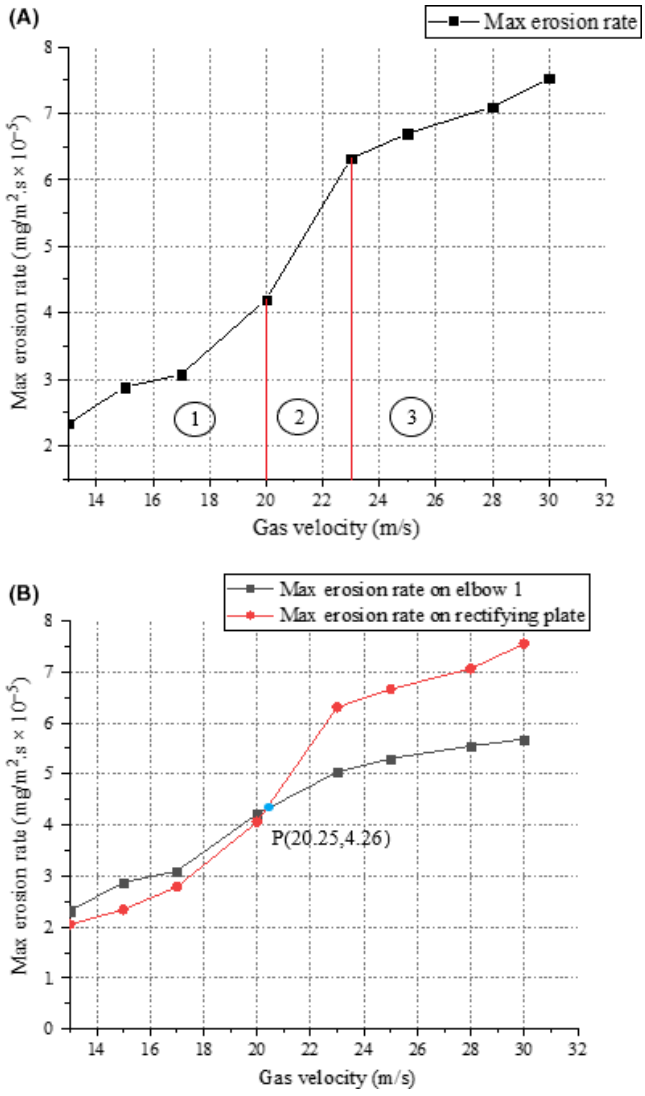

FIGURE 11 A, Max erosion rate of the system under different gas velocities. B, Maximum erosion rates of elbow 1 and the rectifying plate

Figure 13 shows the relationship between the sand input and the maximum erosion rate of the whole system in (A), and it can be observed that the maximum erosion rate increases rapidly when the sand input increases from 150 kg/d to 250 kg/d, and when the sand input exceeds 250 kg/d, the value of the maximum erosion rate of the whole system increases slowly. Hence, in the range of 150-250 kg/d, it is assumed that the influence of the sand input on the whole system is the most obvious. In the Equation (13), the erosion is defined as the sum of erosion per particle in a unit area, and the max erosion rate should change linearly with the sand input. However, larger amount of sand inputted means more particles will be tracked. And because of complex flow field in rectifying plate, the more particles may enter with different angles and the velocity vector of some particles will change. Hence, the max erosion rate will not change linearly with the sand input.

And in (B), two curves in the graph describe the maximum erosion rate on elbow and the rectifying plate, respectively. Two curves almost coincide indicating that the maximum erosion rate of elbow 1 is greatly close to that of the rectifying plate.

The maximum difference between the two curves is about 3×10^{-6} kg/m^2 s which equals to 11.5 mm/y (density of material is 7990 kg/m^3). Because the wall of bundles in the rectifying plate is thin, it is not supposed to use erosion data of the rectifying plate or elbow 1 separately to predict the maximum erosion rate of the whole system under this condition. In order to predict the maximum erosion rate of the whole system, the maximum erosion rate of the rectifying plate and elbow 1 should be measured, compared and predicted by choosing the maximum value.

4.3 | Erosion Analysis at different particle parameters

Different particle causes different erosion. In order to investigate the relationship between particle size, particle shape, and erosion of system, various values of particle diameter and shape factor are set in the simulation as Table 2.

The parameters of sand input and gas velocity are set to 200 kg/d and 20.25 m/s in simulations, respectively. The max erosion rate of rectifying plate system at different particle parameters is calculated, and the results are shown as follow in Figure 14.

As shown in Figure 14, the max erosion rate of system increases slowly with particles diameter ranging from 50 μm to 100 μm. However, when particles diameter increases from 100 μm to 150 μm, the increase in max erosion rate is more obvious. Then, when particles diameter exceeds 150 μm, the max erosion rate almost increases linearly. Moreover, it is found from the results of simulation that when particles diameter changes, the erosion scars distributed in different positions change slightly except the erosion scar on elbow 1. The changes of erosion scar on elbow 1 are shown as follow in Figure 15.

It can be observed that the shape of erosion scar on elbow 1 has a obvious change when diameter of particles increases. At the particle's diameter of 50 μm, the shape of erosion scar is more like an ellipse. With the particle's diameter increasing, the shape of erosion scar changes and the V-shape of it becomes more obvious. To investigate the reason for this phenomenon, the trajectories of particles in elbow 1 obtained from simulation are analyzed and the results are shown in Figure 16.

With increase in the particle's diameter, particles have a tendency to gather when they pass through the elbow 1. However, after hitting the wall of elbow 1, gathered particles disperse in an approximate V-shape along the direction of

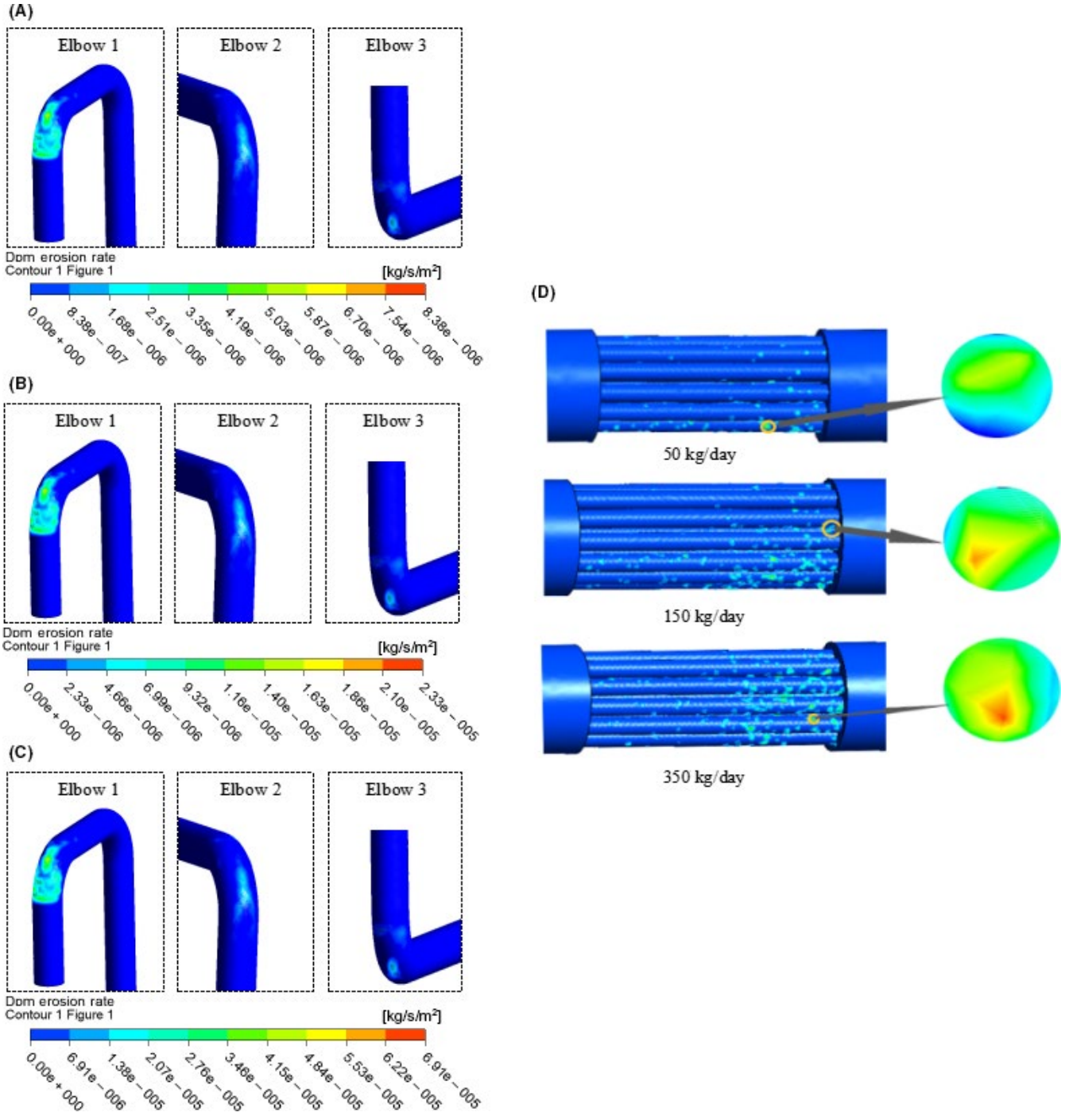

FIGURE 12 A, Erosion rate at the sand input of 50 kg/d. B, Erosion rate at the sand input of 200 kg/d. C, Erosion rate at the sand input of 350 kg/d. D, Erosion rate of rectifying at different sand inputs

airflow. The results of Figure 16 show that the larger particles diameter enhance the particles cluster formation in elbow 1.

Moreover, the relationship between the shape factors and max erosion rate of rectifying plate system has been investigated in this paper. Sand input is set to 200 kg/d, and the gas velocity is set to 20.25 m/s; moreover, the particle diameter is set to 300 μm. The result is shown as follow in Figure 17.

As shown in Figure 17, it can be obtained that when shape factor varies from 1 to 0.9, the max erosion rate of the system changes slightly. Then, with the decrease in the shape factor, the max erosion rate increases gradually. However, when the shape factor decreases from 0.7 to 0.5, the max erosion rate of system increases dramatically. With the shape factor continuing to decrease, the increased tendency of max erosion rate reduced slightly.

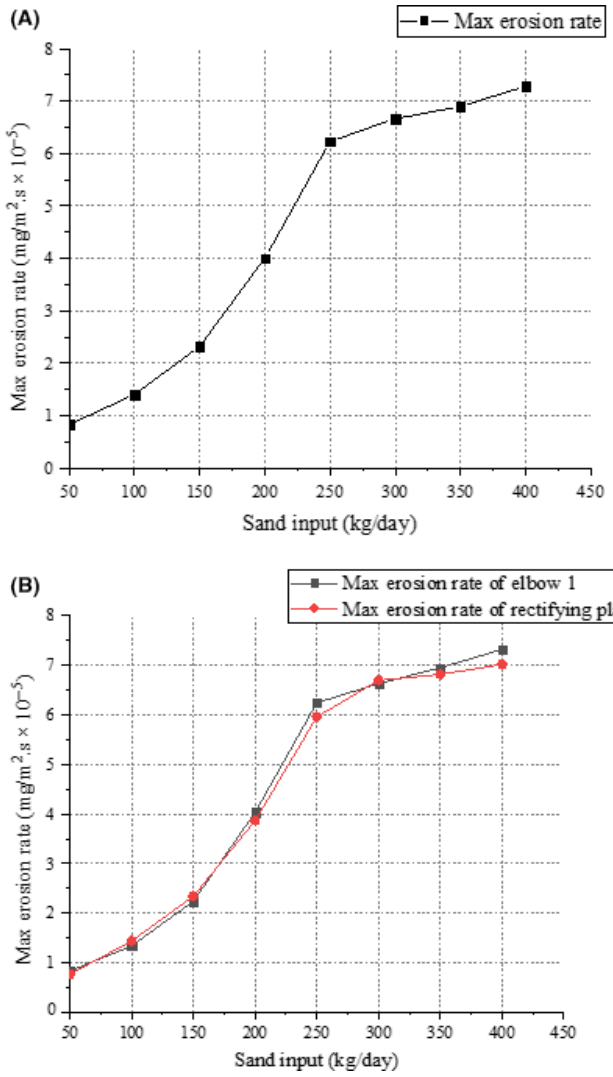

FIGURE 13 A, The max erosion rate of system under different sand inputs. B, The max erosion rates of elbow 1 and the rectifying plate

TABLE 2 Values of particle parameters

Particle parameters	Particle size (μm)	Shape factor
	50	0.4
	100	0.5
	150	0.6
	200	0.7
	250	0.8
	300	0.9

5 | CONCLUSION

The erosion of rectifying system is analyzed in this study. The motion of particles is simulated by using the DPM model, and the effect of flow field on particle trajectory is analyzed

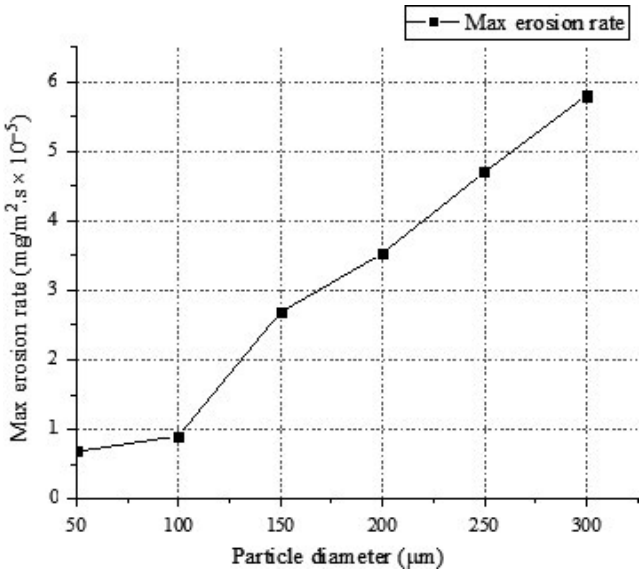

FIGURE 14 The max erosion rate of system under different particle diameters

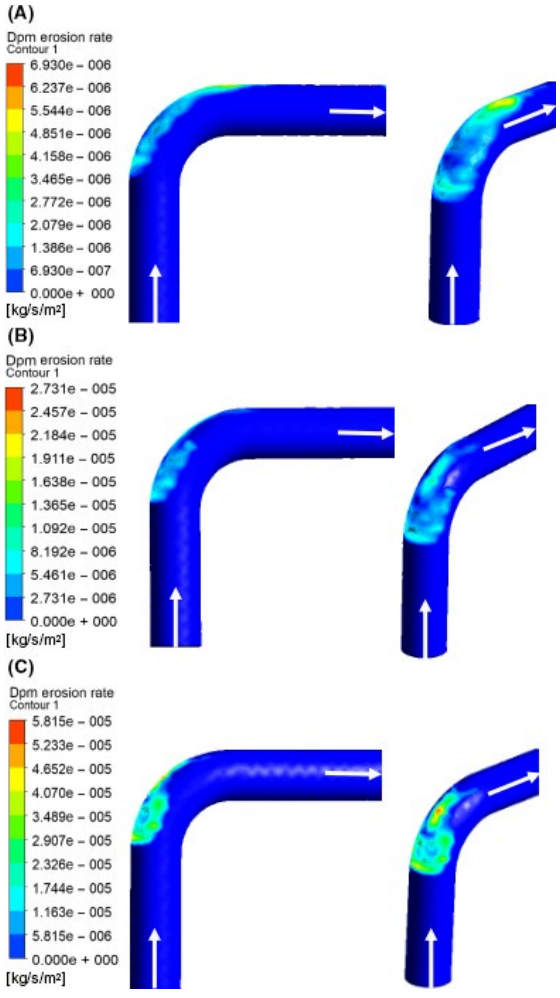

FIGURE 15 The max erosion rate of system under different particle diameters. A, Erosion of elbow 1 at the particles diameter of 50 μm. B, Erosion of elbow 1 at the particles diameter of 150 μm. C, Erosion of elbow 1 at the particle's diameter of 300 μm

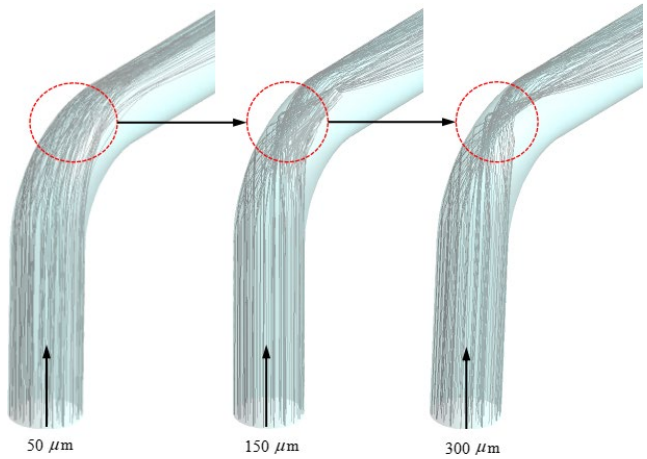

FIGURE 16 Trajectories of particles in elbow 1

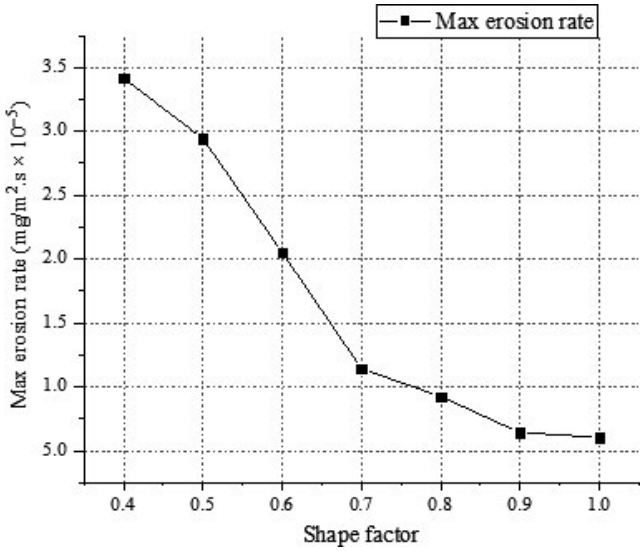

FIGURE 17 The max erosion rate of system under different shape factors of particles

by using finite element method. It is obtained by simulation that various parameters of fluid flow and particles can both affect the erosion in rectifying plate system. However, not only the value of max erosion rate changes, there are some phenomenon is observed from the results of simulation: Gas velocity can affect the position where max erosion rate appears; various particles diameters lead different shapes of erosion scar. Moreover, this study gives a method that under the certain condition, the max erosion rate in rectifying system can be predicted by analyzing the max erosion rate in some necessary positions like elbows or rectifying plate. This method can simplify the detection for whole rectifying system in practical.

This paper fills up the bland in research about erosion in the rectifying system in some certain extent and can provide ideas for relative researches. However, there are still some limitations in this study. Generally, experiment method is the most intuitive reflection of reality. Due to lack experimental instrument, the data of simulation are validated by the data of experiment conducted in Tulsa University. Actually, many factors can affect the accuracy like temperature and air humidity. Moreover, the features of sand particles are more complex in practical which is hard to be completely considered in simulations.

ACKNOWLEDGMENTS

The authors are grateful for the research support received from Applied Basic Research Program of Sichuan Province (2019YJ0352) and Sichuan Provincial Natural Resources Research Project (KJ-2019-11).

CONFLICT OF INTEREST

The authors declare no conflict of interest.

REFERENCES

1. Liu E, Lv L, Ma Q, Kuang J, Zhang L. Steady-state optimization operation of the West-EastGas Pipeline. *Adv Mech Eng*. 2019;11:1-14.
2. Peng S, Liao W, Tan H. Performance optimization of ultrasonic flow meter based on computational fluid dynamics. *Adv Mech Eng*. 2018;10(8):1-9.
3. Duarte C, de Souza FJ. Innovative pipe wall design to mitigate elbow erosion: a CFD analysis. *Wear*. 2017;380-381:176-190.
4. Pei J, Lui A, Zhang Q, Xiong T, Jiang P, Wei W. Numerical investigation of the maximum erosion zone in elbows for liquid-particle flow. *Powder Technol*. 2018;333:47-59.
5. Arabnejad H, Mansouri A, Shirazi SA, McLaury BS. Abrasion erosion modeling in particulate flow. *Wear*. 2017;376-377:1194-1199.
6. Peng W, Cao X. Numerical prediction of erosion distributions and solid particle trajectories in elbows for gas–solid flow. *J Nat Gas Sci Eng*. 2016;30:455-470.
7. Laín S, Sommerfeld M. Numerical prediction of particle erosion of pipe bends. *Adv Powder Technol*. 2019;30(2):366-383.
8. Zeng D, Zhang E, Ding Y, et al. Investigation of erosion behaviors of sulfur-particle-laden gas flow in an elbow via a cfd-dem coupling method. *Powder Technol*. 2018;329:115-128
9. Liu E, Li W, Cai H, Peng S. Formation mechanism of trailing oil in product oil pipeline. *Processes*. 2019;7:7.
10. Duarte C, de Souza FJ, SalvoR, SantosV. The role of inter-particle collisions on elbow erosion. *Int J Multiphase Flow*. 2017;89:1-22.
11. Vieira RE, Mansouri A, Mclaury BS, Shirazi SA. Experimental and computational study of erosion in elbows due to sand particles in air flow. *Powder Technol*. 2016;288:339-353.
12. Duarte C, de Souza FJ, Dos SantosVF. Numerical investigation of mass loading effects on elbow erosion. *Powder Technol*. 2015;283:593-606.
13. Wong CY, Solnordal C, Swallow A, Wu J. Experimental and computational modelling of solid particle erosion in a pipe annular cavity. *Wear*. 2013;303(1-2):109-129.
14. Liu B, Zhao J, Qian J. Numerical analysis of cavitation erosion and particle erosion in butterfly valve. *Eng Fail Anal*. 2017;80:312-324.

15. Yaobao Y, Jiayang Y, Shengrong G. Numerical study of solid particle erosion in hydraulic spool valves. *Wear*. 2017;392-393:174-189.
16. Zhu H, Pan Q, Zhang W, Feng G, Li X. Cfd simulations of flow erosion and flow-induced deformation of needle valve: effects of operation, structure and fluid parameters. *Nucl Eng Des*. 2014;273:396-411.
17. Messa GV, Ferrarese G, Malavasi S. A mixed euler–euler/euler–lagrange approach to erosion prediction. *Wear*. 2015;342-343:138-153.
18. Zhongya S, Enbin L, Yawen X. Flow field and noise characteristics of manifold in natural gas transportation station. *Oil Gas Sci Technol-Revue D IFP Energies Nouvelles*. 2019;74:1-12.
19. Haugen K, Kvernvold O, Ronold A, Sandberg R. Sand erosion of wear-resistant materials: erosion in choke valves. *Wear*. 1995;186-187:179-188.
20. Neilson JH, Gilchrist A. Erosion by a stream of solid particles. *Wear*. 1968;11(2):111-122.
21. Oka YI, Okamura K, Yoshida T. Practical estimation of erosion damage caused by solid particle impact. part 1: effects of impact parameters on a predictive equation. *Wear*. 2005;259(1):95-101.
22. EdwardsJK, McLauryBS, ShiraziSA. Supplementing a CFD code with erosion prediction capabilities. In: *Proceedings of ASME FEDSM'98: ASME 1998 Fluids Engineering Division Summer Meeting, Washington DC*, June 1998.
23. Grant G, Tabakoff W. Erosion prediction in turbomachinery resulting from environmental solid particles. *J Aircraft*. 1975;12(5):471-478.

How to cite this article: Peng S, Chen Q, Shan C, Wang D. Numerical analysis of particle erosion in the rectifying plate system during shale gas extraction. *Energy Sci Eng*. 2019;7:1838–1851. https://doi.org/10.1002/ese3.395